Physics of Fluids

Rheological signatures of aging in hard sphere colloidal glasses

Cite as: Phys. Fluids **31**, 087103 (2019); https://doi.org/10.1063/1.5113500
Submitted: 04 June 2019 . Accepted: 18 July 2019 . Published Online: 14 August 2019

Alan R. Jacob, Esmaeel Moghimi, and George Petekidis

Physics of Fluids ARTICLE scitation.org/journal/phf

Rheological signatures of aging in hard sphere colloidal glasses

Cite as: Phys. Fluids 31, 087103 (2019); doi: 10.1063/1.5113500
Submitted: 4 June 2019 • Accepted: 18 July 2019 •
Published Online: 14 August 2019

Alan R. Jacob,[a] Esmaeel Moghimi, and George Petekidis

AFFILIATIONS

IESL-FORTH and Materials Science and Technology Department, University of Crete, 71110 Heraklion, Greece

Note: This paper is part of the special topic, Invited Contributions from Outstanding Early Career Researchers.
[a]alanjacob88@yahoo.com

ABSTRACT

Colloidal glasses are out-of-equilibrium in nature. When such materials are quenched from a shear-melted state into a quiescent one, their structure freezes due to entropic caging of the constituents. However, thermal fluctuations allow slow structural evolution, a process known as aging, in favor of minimizing free energy. Here, we examine the rheological signatures of aging, in a model system of nearly hard sphere colloidal glass. Subtle changes in the linear viscoelastic properties are detected with the age of the colloidal glass where viscous modulus shows a decrease with aging whereas the elastic modulus remains unaffected. This is associated with the slowing-down of long-time out-of-cage dynamics as the glass ages. On the contrary, nonlinear rheological measurements such as start-up shear flow, stress relaxation, and creep experiments show a strong dependence on sample age. Moreover, creep and stress relaxation experiments show ample evidence of avalanche type processes that occur during aging of colloidal glasses. Finally, comparison of creep and start-up shear flow measurements indicate that the latter is more energy efficient in inducing flow in colloidal glasses irrespective of aging dynamics.

I. INTRODUCTION

Out of equilibrium systems are always driven to a lower free energy state with waiting time[1] and their intrinsic properties such as relaxation time change over time. This process of structural evolution is known as aging.[2] Aging is generally referred to the time elapsed after quenching the system into an out of equilibrium state. In terms of the energy landscape, the system immediately after quenching will have a narrow distribution of shallow energy wells, which with time changes to a broader distribution with deeper energy wells.[3] The concept of physical aging has been investigated for glass former materials.[4–7] There has been a surge of interest in aging of colloidal systems with repulsive or attractive interparticle interactions such as colloidal glasses,[8,9] laponite gels,[10,11] and colloidal depletion gels.[12–16]

Light scattering experiments reported aging dynamics using intermediate scattering functions (ISFs) in purely repulsive hard sphere colloidal glasses.[17–21] A typical ISF for a hard sphere colloidal glass consists of a two-step decay: a fast decay at short times relating to in-cage dynamics and a long-time slow decay also known as alpha relaxation time associated with long-time out-of-cage motion.[20] During aging, alpha relaxation time of hard sphere colloidal glass increases with waiting time initially, but eventually tends to reach a constant value, independent of waiting time.[21] Direct visualization of aging using confocal microscopy on hard sphere colloids[22,23] reveals that glasses exhibit a slowing-down of particle displacements with the sample age. However, gravity also affects the aging phenomena in hard sphere colloidal glasses[22] although this might not be the only reason driving aging. There exists a very close correlation between structural heterogeneities and dynamic heterogeneities during the temporal evolution in a colloidal glass.[24] Computer simulations have also shown that subtle changes in the structural rearrangements lead to aging.[25–27] Moreover, relaxation of internal stresses built-up after quenching from shear-melted to quiescent state have been invoked to explain the slow dynamics and aging in such out-of-equilibrium materials.[28–31]

Identifying rheological signatures of aging in model nearly hard sphere colloidal glasses have been attempted for start-up shear-flow[32] and creep[33] experiments as well as via theory.[34,35] However, comprehensive rheological signatures of aging in colloidal glasses have yet to be explored. Here, we use a model system, of nearly hard sphere colloidal particles, at various particle volume fractions

in the glassy regime to extract unique rheological signatures of aging. We present detailed rheological experiments with a well-defined shear-history in order to elucidate the rheological signatures of aging in colloidal glasses. We demonstrate that aging has subtle effects on the linear viscoelastic properties of the glass. However, discernible changes due to aging are observed when the glass is subjected to nonlinear shear flow like start-up shear flow, stress relaxation, and creep measurements. As discussed above, aging leads to an increase of the intrinsic alpha relaxation time in colloidal glasses. On the contrary, shear was found to accelerate the long-time relaxation in hard sphere glasses.[36,37] Hence, the competition between aging and shear rejuvenation is expected to determine both the structural properties and particle dynamics in colloidal glass.

This manuscript is structured as follows: we first describe the materials used in the study, the rheometry technique, and shear rejuvenation protocol used in experiments (Sec. II). In Sec. III, we start off by presenting the effect of aging on the linear viscoelastic properties of the glass. Later on the aging effects in start-up shear flow, stress relaxation, and creep measurements are presented. Then, we make a comparison between start-up shear flow and creep measurements before and after yielding for aging colloidal glasses. Moreover, we examine the long-time response of colloidal glasses under constant stress (below yield stress) and its link to possible avalanche type processes. Finally, we summarize and make our conclusions in Sec. IV.

II. MATERIAL AND METHODS

We used nearly hard sphere colloidal particles made of polymethyl-methacrylate (PMMA) sterically stabilized by a short grafted layer (≈10 nm) of poly-hydroxystearic acid (PHSA) chains. The colloidal particles of different radius of R = 106 nm, 137 nm, 196 nm and 350 nm were used. Particles have the polydispersity greater than 12% to suppress crystallization. Particles were dispersed in two different solvents: (i) octadecene/bromonapthalene mixture (with viscosity η = 0.0045 Pa s and refractive index n_D = 1.48) and (ii) squalene (η = 0.015 Pa s, n_D = 1.494). Both solvents are closely refractive index matched with particles, and hence, van der Waals attractions are minimized. Moreover, both solvents have a high boiling point (for octadecene/bromonapthalene mixture is 315 °C and for squalene is 421.3 °C) which hinders evaporation and aids long-time rheological experiments.

Anton Paar MCR 501 rheometer has been used for most of the rheological measurements. Additionally, a Rheometric DSR 200 rheometer was also used to perform the long-time creep experiments. In both the rheometers, a cone-plate geometry with diameter 25 mm, a cone angle of 2.71° and a gap size of 0.05 mm was used. Dynamic frequency sweep (DFS) experiments were performed at a low strain amplitude of γ = 0.5% well inside the linear regime.[38] In order to avoid sedimentation, small particles were used for long-time measurements. Our rheological experiments do not show any sign of wall-slip due to sedimentation, usually detected from the flow curves via the observation of a clear second pseudoyield stress plateau from which the slip stress can be determined,[39–41] as seen in Fig. 1(b). Moreover, the experiments for steady state flow conditions lies in the nonshear banding regime for steady state flow based on prior rheo-confocal experiments[42] on hard sphere colloidal glasses, although we cannot exclude the existence of transient shear banding during creep at low stresses, below the yield stress.

A. Shear rejuvenation protocol

Two types of shear rejuvenation protocols are employed depending on the volume fraction ϕ in order to avoid shear thickening and edge fracture in glassy colloidal suspensions. Colloidal glasses with $0.58 \leq \phi \leq 0.60$ were rejuvenated with a large strain amplitude of γ = 100% and frequency of 1 rad/s. Above ϕ = 0.60, the system was rejuvenated at a lower frequency of 0.1 rad/s. Then, the system was allowed to age at zero stress for the required waiting time before each measurement was conducted.

III. RESULTS AND DISCUSSION

A. Aging effects on linear viscoelastic properties

We begin by presenting the typical linear viscoelastic frequency sweep of a colloidal glass [Fig. 1(a)]. The trivial size effects of the colloidal particles are removed by scaling the moduli by entropic energy, k_BT/R^3, since Brownian forces are the sole contributor to the elasticity. The nondimensional Péclet number $Pe = \dot{\gamma}t_B$, the product of the shear rate and the Brownian time, t_B, represents the relative importance of the shear flow to Brownian motion. In oscillatory experiments, $Pe_\omega = \omega t_B$ is used instead, where ω is the angular

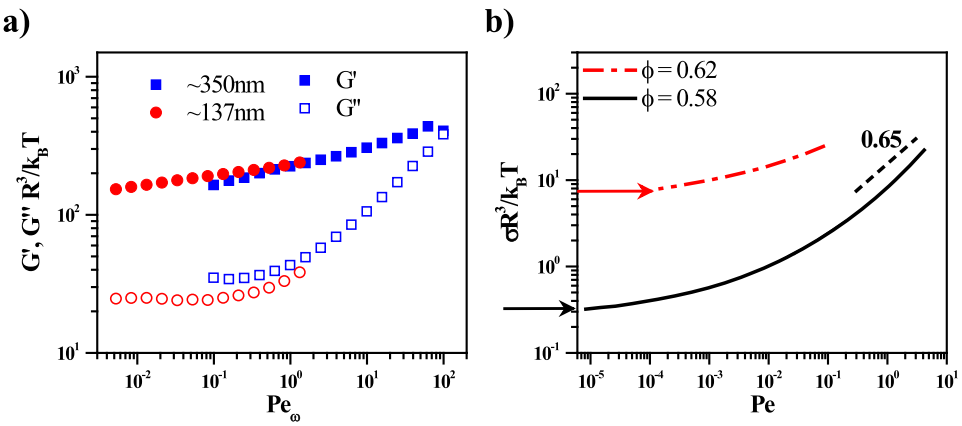

FIG. 1. (a) The Pe_ω dependence of storage G' and viscous G'' moduli for a hard sphere colloidal glass with ϕ = 0.61 in octadecene/bromonapthalene mixture with 350 nm (square) and 137 nm (circle). The elastic modulus G' is shown by closed symbols and the viscous modulus G'' by open symbols. (b) Steady state shear stress as a function of Pe (flow curve) for hard sphere colloidal glasses for ϕ = 0.62 (solid line) and ϕ = 0.58 (dashed-dotted line) with colloidal particle radius R = 106 nm in squalene. The horizontal arrows indicate the yield stress values.

frequency. Here, Brownian time is calculated in the dilute regime as $t_B = 6\pi\eta R^3/k_BT$ where k_B is the Boltzmann's constant and T is the temperature. Two different particle sizes are compared at the same particle volume fraction, $\phi = 0.61$. This provides access to a wider Pe_ω range in the viscoelastic spectrum. In Fig. 1(a), the values of elastic modulus, G', superimpose quite well for both particles while for viscous modulus, G'', some mismatch is observed near the minimum of G'' ($0.3 < Pe_\omega < 1$). The latter might be due to difference in the scaled aging time, t_w/t_B, time between the colloidal glasses comprising different particle sizes, as the t_w was kept at ≈100 s in both cases. In this scenario, the small particles age more compared to big particles for the same experimental time by a factor of: $t_{Bbig} = 16.67t_{Bsmall}$. At high Pe_ω (≈100), the upper limit of the experimental frequency window, a crossover between G' and G'' is detected, above this crossover the time scales are associated with in-cage particle vibrations. For Pe_ω below crossover (<100), however, G' shows larger values compared to G'' indicative of a solidlike response. This is a typical response in a variety of soft-glassy materials where G' shows a gradual increase with frequency whereas G'' exhibits a minimum.[43] This elastic modulus dominance over the Pe_ω relates to time scales where the particle is constrained due to the cage formed by the neighboring particles. Next, we examine the mechanical response of the glasses under a well-developed steady state shear flow. Figure 1(b) shows the steady state values of shear stress as a function of Pe (flow curve) for the particle volume fractions near and well above the glass transition. The flow curve shows the general response expected for concentrated colloidal glasses. At low Pe ($<10^{-2}$), a yield stress plateau emerges, with yield stress increasing with particle volume fractions. As Pe is increased, stress exhibits a sublinear growth with Pe which indicates shear-thinning of the viscosity, i.e., a decrease of the effective viscosity. This is due to the diminished Brownian contribution and possible alignment of particles in the flow direction which reduces viscosity.[44,45]

We present the effect of aging on the linear viscoelastic properties of the glass. Figures 2(a) and 2(b) show the time evolution of both elastic and viscous moduli after shear rejuvenation for two different volume fractions of $\phi = 0.58$ and $\phi = 0.62$. For both volume fractions, the elastic modulus shows essentially no change over time, whereas a subtle decrease is detected for the viscous modulus with the higher volume fraction glass showing a weaker time evolution. The latter could be associated with smaller free volume available for particles at higher volume fractions to rearrange and find a minimum in energy landscapes. More insight emerges when the linear viscoelastic spectrum of the glass at different aging times after shear rejuvenation is examined [Figs. 2(c) and 2(d)]. Aging does not affect G' for the Pe_ω range examined here, whereas G'' decreases mainly at low Pe_ω as the glass ages. This is in agreement with previous findings in similar hard[33] and soft[46] sphere colloidal glasses. G'' shows a minimum at low Pe_ω, which represents the time scale that separates fast in-cage dynamics (β relaxation) from the ultraslow (or completely frozen) out-of-cage motion (α relaxation). The in-cage dynamics are not affected by aging and hence high frequency values of G'' are the same independent of age. However as the glass ages, any long time structural rearrangements present slow down.[19,21] This shifts the minimum of G'' to lower Pe_ω and hence leads to a decrease in G'' at low Pe_ω with increasing sample age.

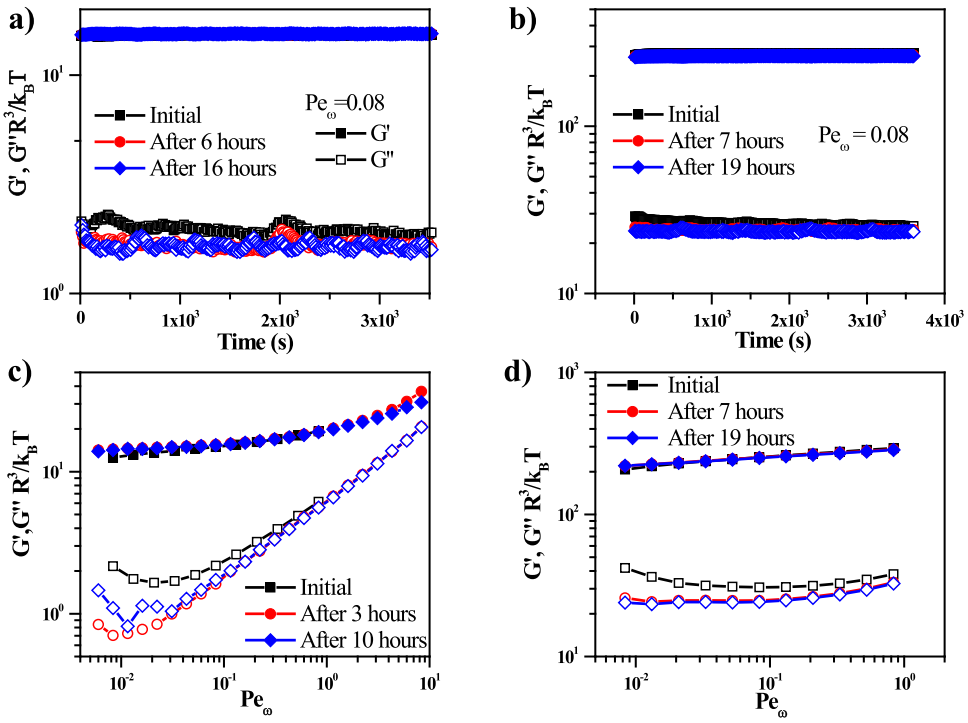

FIG. 2. Time evolution of elastic G' (closed symbols) and viscous G'' (open symbols) moduli for a period of 1 h at different aging times after shear rejuvenation as indicated for (a) $\phi = 0.58$ and (b) $\phi = 0.62$ with colloidal particles of $R = 106$ nm dispersed in squalene. Dynamics frequency sweeps (DFS) for the glass with (c) $\phi = 0.58$ and (d) $\phi = 0.62$ after various aging times. The y-axis moduli are scaled by thermal energy density (k_BT/R^3) and the x-axis frequency scaled by Brownian time (t_B).

B. Nonlinear rheology: Aging effects on start-up shear flow and stress relaxation measurements

We now discuss the effect of sample age on the start-up shear flow experiments. In such transient tests, a constant deformation rate (shear rate) is applied and the evolution of stress with time or accumulated strain ($\gamma = \dot{\gamma}t$) is monitored. A typical start-up test for a hard sphere colloidal glass with $\phi = 0.58$ at two different aging times is shown in Fig. 3(a). With the application of shear flow, initially stress shows an almost purely elastic response with a sublinear increase due to the existence of finite viscous contribution which is followed by a stress overshoot when strain reaches a value of about 10%, which finally decays towards a steady-state plateau at larger strains ($\gamma > 50\%$). The initial stress growth represents an energy storage mechanism associated with elastic deformation of the cage, whereas the stress peak reflects a subsequent energy dissipation related to cage breaking that leads to plastic flow and a constant steady state stress.[32,47] This kind of plastic deformation is also observed during large amplitude oscillatory shear flow.[48,49] When the glass is sheared, particles come closer along the compression axis under flow while they are pushed outward along the extension axis. This causes a progressive structural anisotropy during start-up shear flow which decreases after the stress peak leaving behind a considerable anisotropy in the steady-state.[32,47] As the colloidal glass ages, an increase in value of stress overshoot during start-up shear flow is observed. However, the age-dependence of stress overshoot diminishes for start-up shear experiments performed at high *Pe*.[32] This indicates that at low *Pe* aging dominates over shear rejuvenation, whereas at high *Pe* shear-induced rejuvenation counteracts aging. Similar dependence of stress overshoot with sample age have been observed in PS-PNIPAM core shell particles and discussed in the framework of Mode Coupling Theory (MCT).[34] Aging of a colloidal glass mainly manifests in the stress overshoot peak, while the short-time response as well as the final steady state stress is independent of aging. The age-independence of steady state shear stress indicates a unique shear-melted state where the structural history created during aging has been completely erased by shear flow.

Next, we examine stress relaxation after flow cessation at different times/strains during start-up shear flow measurements for two different aging times. The stress decay is normalized by its value just before flow interruption as shown in Fig. 3(b). As the accumulated strain increases, fluidization is enhanced as the structural relaxation time becomes faster. Hence, when flow is stopped, particles move faster and relax the stresses much more before dynamical arrest due to particle caging sets in. This is analogous with flow cessation after steady shear, where faster and stronger stress decays are observed after flow cessation for higher shear rates.[50,51] In general, the older samples retain more stresses during the stress relaxation [Fig. 3(b)]. Aging of a colloidal glass slows down the relaxation time[19,21] increasing its capability for storing energy, also shown by the increasing peak of shear stress in Fig. 3(a). However, the effect of aging on stress relaxation reduces when the applied strain during start-up shear increases and for $\gamma = 100\%$, where a full shear rejuvenation has been achieved, aging effects diminishes. It should also be noted that some kinks are observed during stress relaxation which will be discussed later.

Another way to perform stress relaxation experiments is by imposing a step-strain. Figure 4 shows the stress relaxation at various aging times for step-strain measurements in the linear and nonlinear regimes, i.e., at strains well below and above the yield strain, respectively. When the applied step-strain is small (for example, $\gamma = 1\%$, well inside the linear regime), the younger sample (with $t_w = 100$ s) releases the stress quickly like a viscoelastic fluid [Fig. 4(a)]. As mentioned earlier, younger glasses have shorter relaxation times, hence, when a step-strain is imposed, they relax the stress faster. However, the age-dependence of stress relaxation is significantly reduced when a large step-strain, $\gamma = 50\%$ is imposed [Fig. 4(b)]. This is a clear indication that a partial shear rejuvenation has occurred in the sample. The stress relaxation measurements provide ample evidence that the internal relaxation time increases with waiting time. Recently, a soft glassy material (SGM) model was proposed which considered aging and shear rejuvenation as a decrease and increase of the free energy, respectively.[35] The model predicts the existence of residual stresses when the relaxation time exhibits a superlinear dependence with waiting time. Light scattering experiments on hard sphere colloidal glasses demonstrate a dependence of the alpha relaxation time with waiting time as well.[21] Hence, our rheological experiments combined with light scattering data published earlier seems to support the modified SGM model predictions.

In Figs. 4(c) and 4(d), we present the stress relaxation experiments after imposing step-strain for the glass with a higher particle volume fraction, $\phi = 0.63$. The overall observation is similar to a lower volume fraction of $\phi = 0.6$: as the glass ages, it retains more

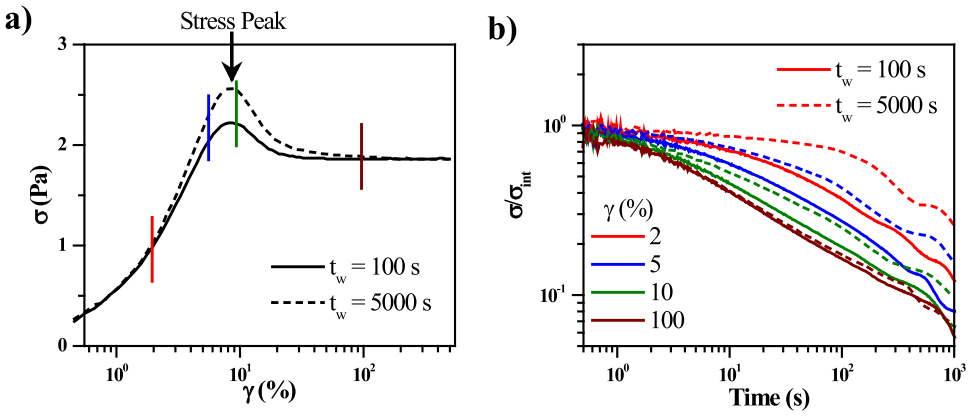

FIG. 3. (a) Start-up shear flow experiments performed at $Pe = 8.33 \times 10^{-4}$ for two waiting times of $t_w = 100$ s (solid line) and $t_w = 5000$ s (dashed line). (b) The stress at the time of shear cessation of start-up shear at various strains as indicated in the legend. The stress has been scaled by the corresponding value, σ_{int}, at the time of flow interruption. The colloidal system represented here have $R = 106$ nm suspended in squalene with $\phi = 0.58$. The vertical lines in (a) indicate the strain at which flow is interrupted.

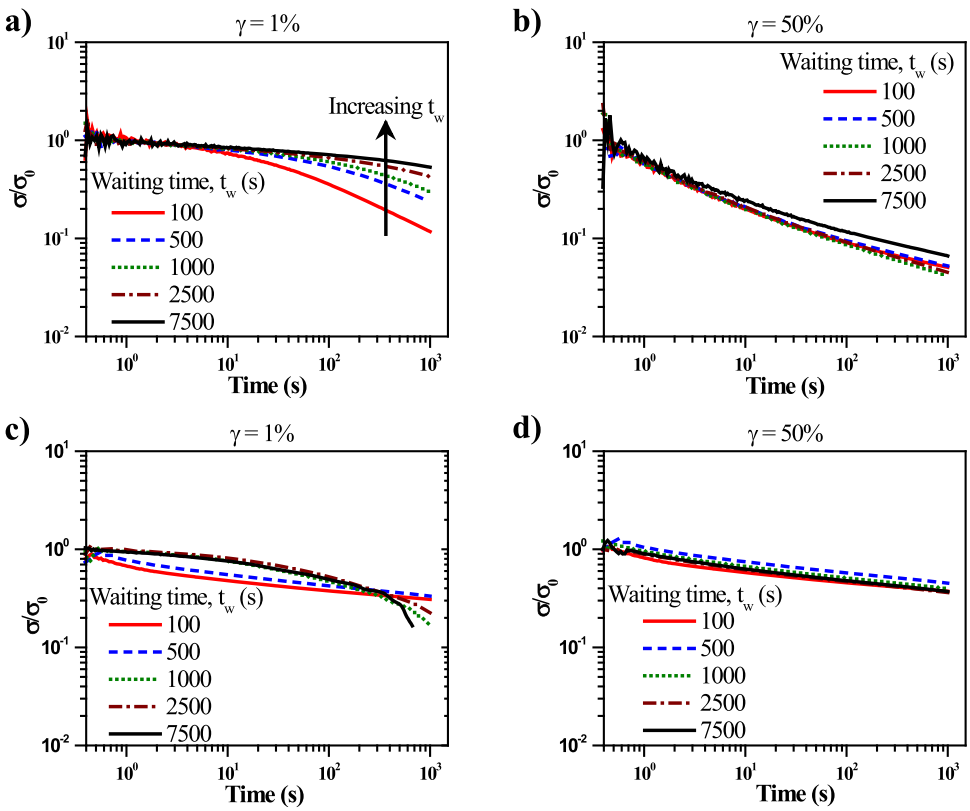

FIG. 4. Stress relaxation data for colloidal glass (R = 196 nm) in octadecene/bromonapthalene solvent mixture with a volume fraction $\phi = 0.6$ at step-strain of (a) $\gamma = 1\%$ and (b) $\gamma = 50\%$ for waiting times 100 s (solid red line), 500 s (dashed blue line), 1000 s (dotted green line), 2500 s (dashed-dotted brown line) and 5000 s (solid black line) after shear rejuvenation. Stress relaxation for (c) $\gamma = 1\%$ and (d) $\gamma = 50\%$ for a glass with $\phi = 0.63$ and particle radius R = 106 nm.

stresses after imposing step-strain. Moreover, the stress relaxation becomes less sensitive to aging as the imposed step-strain is increased. Specifically in Fig. 4(c) the step strain of $\gamma = 1\%$ for high volume fraction glass $\phi = 0.63$ is closer to the yield strain hence the two different relaxations patterns can be observed. At small waiting times (t_w = 100, 500 s), the stress relaxation is similar to that above the yield stress. For $t_w > 500$ s, the glass ages sufficiently to show response similar to Fig. 4(a). However, for such high volume fraction glass $\phi = 0.63$ and large waiting times, the stress decay at long-times often exhibits a kink, for example, $t_w = 7500$ s. Such sudden decay in stress at long-times may be associated with avalanche type local particle rearrangements that propagate within the sample during stress relaxation. Computer simulations have reported the occurrence of subtle changes in configuration space during aging.[25,26] This phenomenon could lead to sudden drops in the stress for aged samples during stress relaxation. We also observe that these kinks disappear when a step-strain beyond the yield strain is applied [Fig. 4(d)]. In the linear regime, aging drives the colloidal system into deeper energy minima in the energy landscape. Thus, subtle fluctuations in particle position could lead to drastic cooperative local rearrangements leading to sudden drops in stress. On the other hand, when step-strain beyond the yield strain is applied, all particles are pushed to more shallow energy minima, as the system is partially (or fully) rejuvenated which aids in rearrangements on larger length scales spanning the whole available space. A more detailed discussion on the long-time response and its connection to avalanches will be presented later.

C. Nonlinear rheology: Aging effects during creep experiments

In creep experiments, a constant stress is applied on the sample and the evolution of strain, $\gamma(t)$, with time is probed. Experiments and simulations demonstrate that the macroscopic deformation of the glass is linearly linked to microscopic single-particle mean-squared displacements.[52] Hence, the strain measured in creep experiments reflects the particle dynamics under constant stress. In Fig. 5, we present the strain evolution, $\gamma(t)$, upon imposing various step-stresses for a colloidal glass with $\phi = 0.61$. For all stresses, the strain shows an initial fast growth for $t < 0.1$ s followed by resonant "creep ringing" that arises from an interference of the motor inertia with the sample elasticity.[53] Beyond this regime and for $\sigma < \sigma_y$, $\gamma(t)$ shows a plateau which is followed by a weak sublinear increase at longer times. Microscopic imaging in this regime indicates the existence of heterogeneous active localized domains with nonaffine subdiffusive dynamics.[52] Moreover, dynamic light scattering experiments indicate a progressive slowing down of the intrinsic long-time relaxation as the sample ages under stress.[33] However, above the yield stress ($\sigma_y R^3/k_B T = 2.54$), the strain exhibits a progressively faster increase, reaching a linear dependence with time, a steady state regime with constant viscosity. In Fig. 5, the steady state flow regime is not reached immediately when a critical yield strain is above $\sigma R^3/k_B T \gtrsim 2.54$. Rather, a smooth transition from a sublinear response below the yield strain to yielding and flow above the yield strain, in contrast to delayed yield phenomena observed in colloidal

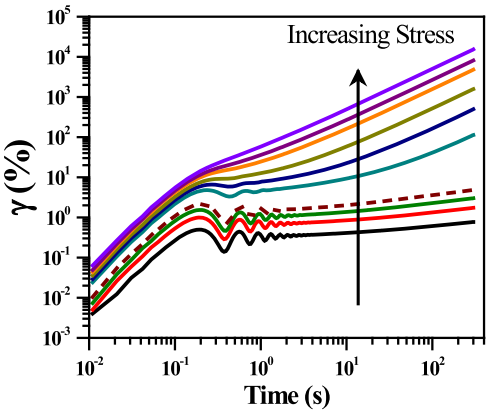

FIG. 5. Representative creep curves for colloidal glass at various step-stresses scaled by thermal energy (with stress, $\sigma R^3/k_BT$ = 0.64, 1.27, 1.91, 2.54, 5.09, 6.36, 7.63, 9.53, 10.81, 12.72 from bottom to top) with yield stress $\sigma_y R^3/k_BT$ = 2.54 (dashed line) for ϕ = 0.61 and colloidal particle radius R = 137 nm in octadecene/bromonapthalene solvent mixture. For all the creep curves, the waiting time was maintained at t_w = 100 s.

gels or other thixotropic materials.[54] Previous studies suggest that microscopically, on application of $\sigma > \sigma_y$, localized active domains in the glass start to grow heterogeneously with particles showing super diffusive dynamics that ultimately leads into diffusive dynamics and flow of the glass.[52]

Next, we examine the effect of sample age on the yielding behavior of colloidal glasses during the creep measurements. As seen in Fig. 6, the older glass (left to age at rest) creeps for a longer period of time before it reaches a steady state flow with constant viscosity. The creep ringing is not affected by aging, in agreement with the weak dependence of the linear viscoelastic spectra with waiting time. Moreover, the long-time behavior where flow sets in is also not affected by the sample age similar to findings in start-up shear experiments [see Fig. 3(a)]. In order to clearly identify the transitions between different strain regimes during creep experiments, a logarithmic derivative of the strain with respect to time is calculated as $\lambda = \frac{d\log(\gamma)}{d\log(t)}$ with $\gamma \sim t^{\lambda}$ as introduced previously.[55] For $t < 10$ s, where creep ringing is observed, data appears scattered and hence is not shown in Fig. 6(b). Immediately after ringing, λ shows an increase with respect to time and reaches a value of 1 at time t_1 [open square symbols in Fig. 6(b)]. This time marks the transition from the creeping regime where strain grows sublinearly with time i.e., $\lambda < 1$, to the super-linear regime ($\lambda > 1$). This is followed by a maximum in λ at t_{max} [open circle symbols in Fig. 6(b)] and finally a decay toward a steady-state flowing regime with $\lambda_{flow} = 1$ where γ grows linearly with time. The transition time from creep regime to super-linear regime (t_1) shifts to longer times with aging. This is a result of slowing down of the relaxation time with sample age. Moreover, for the younger glass the value of λ_{max} is smaller and takes place at shorter times. This suggests that the younger glass yields faster and exhibits a weaker superlinear transient response under constant stress. This is reminiscent of the weaker stress overshoot observed in younger samples in transient step rate tests. After the peak in λ, the younger sample also reaches the flow regime earlier.

D. Stress vs strain controlled shear experiments

Next, we contrast the findings from creep experiments with those from start-up shear measurements. Although both experiments are expected to reach the same final steady flow conditions, the path followed toward the final state is different.[55] In order to compare both measurements, the product of stress times shear rate, $\sigma\dot{\gamma}$, is plotted against time. In Fig. 7, we show comparative plots of strain controlled (start-up shear flow) and stress controlled (creep) measurements for two values of stress/shear rate at various waiting times after shear rejuvenation. The applied stress values for stress controlled measurements are greater than yield stress, σ_y. The values of shear rate for start-up shear tests and the values of stress for creep experiments are chosen in such a way that the superposition of $\sigma\dot{\gamma}$ during steady state is reached. This means that the shear rate reached under constant stress is the same with the one applied at a step rate experiment, or equivalently the stress measured in the latter at steady state is the same with the one applied in the creep test. In start-up shear experiments, a clear stress overshoot is observed for both shear rates, becoming more pronounced with

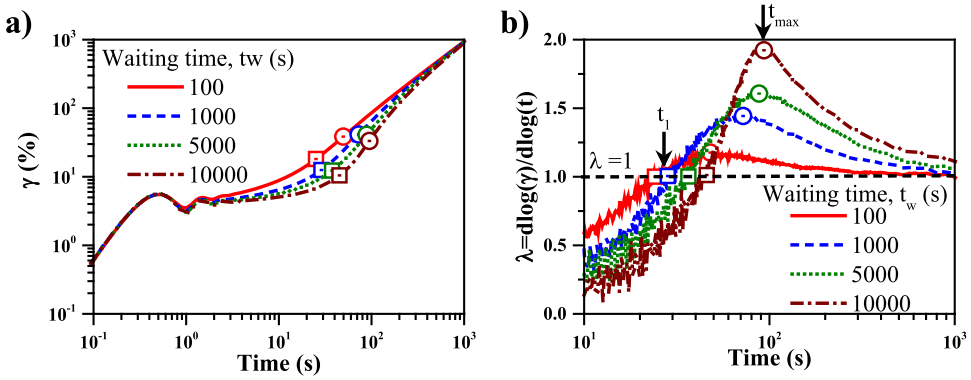

FIG. 6. (a) The time evolution of the strain during creep experiments with σ = 1.86 Pa ($\sigma R^3/k_BT$ = 0.56) at different sample ages. The waiting times, t_w are 100 s (solid line), 1000 s (dashed line), 5000 s (dotted line), and 10 000 s (dashed-dotted line). (b) The logarithmic derivative of the strain with respect to time λ calculated from the creep data in (a). The open squares indicate the time t_1 where λ = 1 and the open circles indicate t_{max} where λ has reached its maximum value. Data shown for hard sphere colloidal glass with ϕ = 0.58 in squalene. The horizontal dashed line indicates λ = 1.

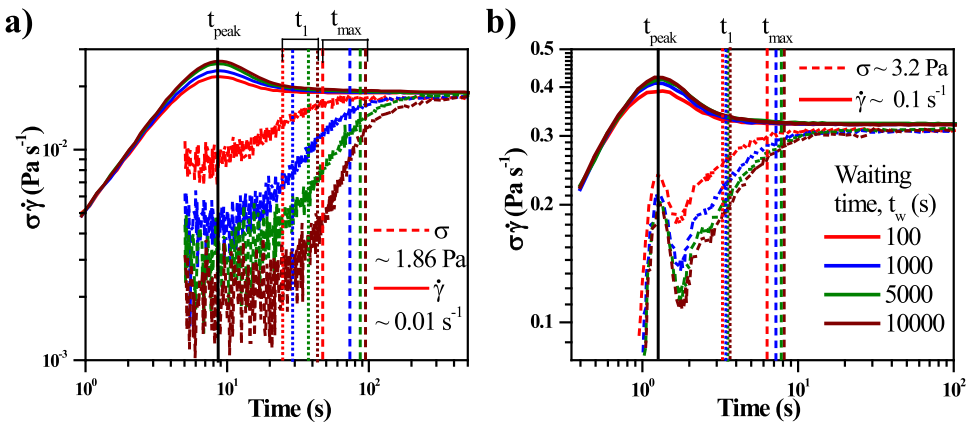

FIG. 7. Comparison between creep (dashed line) and start-up shear (solid line) measurements for ϕ = 0.58 at (a) $\dot{\gamma}$ = 0.01 s^{-1} and σ = 1.86 Pa and (b) $\dot{\gamma}$ = 0.1 s^{-1} and σ = 3.2 Pa. The vertical solid line indicates t_{peak}, the dotted line t_1, and the dashed line t_{max} for different sample ages.

age, as expected.[32] After yielding, the system begins to flow reaching a constant steady state stress independent of aging time. It is difficult to discern the time required to reach steady state flow in stress (creep) test. As the glass ages, it creeps for a longer period of time before reaching steady state flow. In Fig. 7, we superimpose different time scales (shown as vertical lines in Fig. 7) on the creep and start-up curves to evaluate the aging effects on the onset of flow in the two types of transient tests. In the start-up experiment, we define t_{peak} at the maximum of the stress overshoot which as we see here and in Fig. 3 it remains essentially unaffected by aging. The time scales in creep as defined earlier (see Fig. 6) are a function of sample age. Additionally, in Fig. 6(a) for σ = 3.2 Pa the time scales, t_1 and t_{max}, have a smaller spread compared to σ = 1.86 Pa in Fig. 6(b). This is a clear indication that aging affects the time scales in creep much more drastically than start-up shear.

In Fig. 8, we plot the time scales extracted from the step rate and creep measurements from Fig. 7. t_{peak} is the time corresponding to the peak stress overshoot, σ_{peak}, for strain rate controlled experiments, while t_1 and t_{max} are the times where λ reaches 1 and maximum, respectively, for the stress controlled experiments. Interestingly, t_{peak} in the strain rate controlled experiment does not seem to change with aging time irrespective of the applied shear rate, as

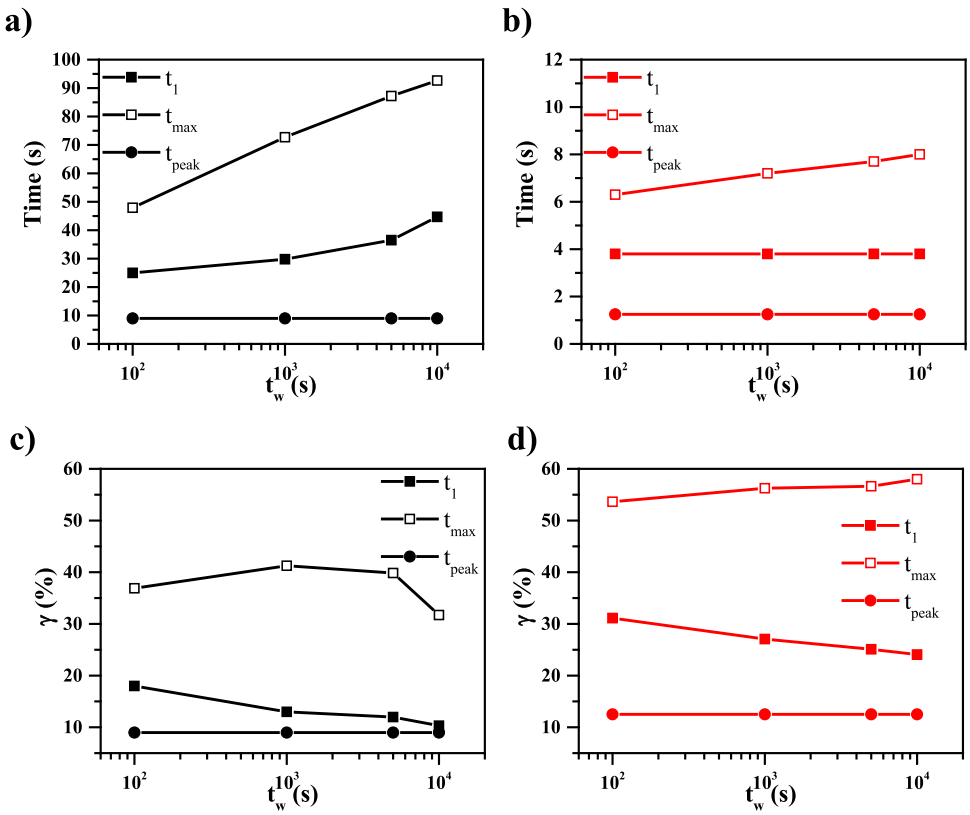

FIG. 8. The age dependence of t_1 and t_{max} from creep experiments and t_{peak} from step rate measurements obtained from Fig. 7 for a hard sphere glass with ϕ = 0.58 for (a) $\dot{\gamma}$ = 0.01 s^{-1} and σ = 1.86 Pa and (b) $\dot{\gamma}$ = 0.1 s^{-1} and σ = 3.2 Pa. (c) and (d) indicate the corresponding strains related with the times presented in (a) and (b), respectively.

mentioned above. Only the strength of the stress overshoot peak is affected by aging [see Figs. 3(a) and 7]. The characteristic times t_1 and t_{max} in creep experiments show an increase with the sample age for σ = 1.86 Pa [Fig. 8(a)]. t_{max} shows a weaker dependence on the sample age as shear stress is increased to 3.2 Pa, whereas t_1 exhibits subtle dependence as shown in Fig. 8(b). This can be understood in terms of the competition between aging and shear-induced rejuvenation. With increasing shear rate and/or shear stress, the intrinsic relaxation time which is affected by sample age becomes less important and shear-induced particle collisions start to be dominant leading yielding. In general, the characteristic time of step-rate experiments, t_{peak} is shorter compared to those from creep measurements. In both creep and start-up shear experiments, larger stress or shear rate leads to yielding and flow at shorter times. This is related to a faster cage escape of particles as a stronger flow field is applied.[32,47]

Now, we define the energy density (energy per unit volume) required to induce yielding and flow in both stress and strain controlled measurements as $\int_{t_o}^{t_n} \sigma\dot{\gamma}dt$, where t_o is the time at the beginning of the experiment and t_n indicates t_1, t_{max} for stress controlled experiments or t_{peak} for the strain controlled experiments. The energy determined in this way is the area under the curve in Fig. 7 with the time limits described above. Results of such analysis are shown in Fig. 9. For start-up experiments, the required energy shows a slight increase with the sample age. This is a result of the transient stress enhancement (increase of the stress overshoot) during the start-up test as the glass ages (see Fig. 7). In creep experiments, the energy per unit volume calculated up to t_1 decreases with sample age irrespective of the applied stress. Interestingly, the energy required for the upper limit t_{max} to be reached is approximately 2 times larger than that required in start-up experiment and creep up to the limit t_1. A positive slope in energy is observed for the upper limit of t_{max} which also suggests that more energy is required to make an aged colloidal glass to yield.

Part of the energy input in the system is elastically stored by deforming the microstructure (cage) and may therefore be returned back in the form of strain recovery during a stress cessation (recovery after creep) experiment. This is demonstrated by the linear increase of the recovered strain (in a creep and recovery experiment) up to the yield stress and its subsequent leveling off to a plateau value that can be identified with the yield strain, as observed in previous studies.[56,57] Microscopically, this is related to continuous cage breaking and reformation and a deformed structure in the shear-gradient plane which relaxes upon shear cessation.[32,50] Since experiments in Figs. 7 and 8 take place above the yield stress with the system yielding and flowing, a part of the provided energy is dissipated through plastic deformations, related to irreversible particle rearrangements and successive cage breakage and reformation.[32] The elastic part should then correspond to the energy input up to the maximum structural deformation or the yield point (around t_{peak} in a start-up shear or t_1 in a creep test) and can be retrieved as a strain recovery upon stress removal (after a creep experiment) or as a stress relaxation upon shear cessation (after a steady shear experiment). Hence, we expect that most of the energy density provided to the system until t_{peak} or t_1 to be mainly of elastic character and to be recovered upon shear cessation, while the one related to t_{max} should include a larger dissipative, thus unrecoverable part. It is only after the t_{max} that the colloidal glass begins to flow approaching a steady state viscosity as it is evident from Fig. 6. As the glass ages its relaxation time slows down and therefore increases its resistance against deformation when it is subjected to a constant stress. Hence, an older glass shows a lower transient shear rate (deformation rate) during creep experiments [see Figs. 7, 8(c), and 8(d)] which subsequently leads to a lower value of the energy per volume introduced to the system. Therefore, under constant stress the time needed to fluidize the system is higher for an aged sample due to its evolution to inherent lower energy minima (and internal relaxation times) that take more time to be rejuvenated (fully or partly, depending on the level of the stress) by shear. On the other hand when a constant shear rate is imposed, the internal relaxation time is essentially fixed by shear and therefore t_{peak}, the time the sample yields, is not affected by age; its rather the stress that increases, for a constant rate the stress needed to yield an aged sample (with inherently lower energy minima and larger internal relaxation times) is larger. Hence, the two phenomena, the increase of the transient stress overshoot at constant rate and the decrease of the transient shear rate (or increase of time for yielding) under constant stress, with increasing age, are interconnected.

The differences observed in characteristic times and energy density in creep and start-up shear experiments (Figs. 8 and 9) can be related to the difference in the nature of yielding in the two tests. In shear-rate controlled experiments, the activation of cage breakage occurs at once all throughout the sample[32,47] whereas in creep test, activated local domains are known to exist in the glass that grow with time until flow sets in.[52] Hence, in start-up shear flow

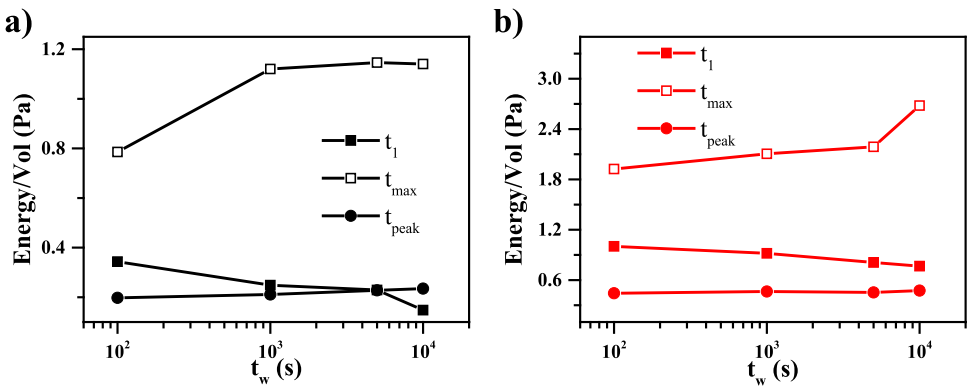

FIG. 9. The energy density induced in the system until the specific time t_n as a function of the waiting time after shear rejuvenation for hard sphere colloidal glass with ϕ = 0.58 for (a) σ = 1.86 Pa, $\dot{\gamma}$ = 0.01 s^{-1} and (b) σ = 3.2 Pa, $\dot{\gamma}$ = 0.1 s^{-1}.

experiments particle dynamics is faster which subsequently leads into a faster yielding and flow with less required work compared to creep measurements. From the above discussion, it can be inferred that a strain controlled experiment is more energy efficient in inducing flow in the sample than a stress controlled experiment.

E. Long-time creep measurements

Finally, we examine the long-time response in creep measurements and its link to possible avalanche type events that manifests during such experiments. Computer simulation on amorphous solids demonstrated the appearance of dynamic noise in the stress during steady shear flow.[58–62] Such fluctuations are directly correlated with the cascading quadrapolar events or avalanches taking place during steady state flow. An entire three dimensional mapping of ice crystals subjected to a constant load relates the plastic flow to dislocation avalanches.[63] This avalanche type flow behavior has been observed during flow of yield stress fluids also.[64] The avalanche process in such fluids, defined as the process where fluid starts flowing abruptly and start to accelerate. Microscopically, this kind of process has been speculated to be the unjamming of the jammed system. Moreover, avalanches are known to mediate crystallization during aging at rest of hard sphere colloidal glasses.[65]

In Fig. 10, we present the long-time response of a colloidal glass under the application of constant stress. Initially, the sample was shear rejuvenated and then allowed to age for two different waiting times of 100 s and 7200 s. A stress of $\sigma = 0.25$ Pa, below the yield stress, $\sigma_y = 2$ Pa, was applied for the duration of 3×10^4 s. In Fig. 10, we observe the effect of waiting time on the creep test as shown earlier.[33] An interesting finding is the appearance of sudden jumps in the strain for the younger glass. We should note that both the total strain reached at long times and the strain jumps are around 1%. Therefore, the latter represents a temporary yielding of the glass as after the jump the strain flattens again which means the glass stops flowing. The low value of strain plateau for low stresses (below the yield stress) corresponds to the elastic regime. This counterbalances the externally imposed stress by the internal stress (or internal anisotropic osmotic pressure) built due to the deformation of the structure which driven by entropy (or Brownian motion) is constantly pushed back to equilibrium. The low value of strain jump itself indicates that the microscopic origin of such temporary yielding is not cage breaking. If the cage escape of particles was the origin for such strain jump, the values should have been around 10%–20%, related to the typical cage size deformation at yielding (or with the distance between particles at these volume fractions). Hence, such short length scale events, manifested as temporary yielding, may originate from rare yielding events of localized cooperative particle rearrangements (or localized slip between particles) which trigger nearby motion and eventually propagate, like avalanches, throughout the gap in order to cause a small macroscopic deformation of the sample measured in the rheometer as a small strain jump. Note however that the above picture holds provided that the whole sample is uniformly strained. In case only part of the sample is sheared (i.e., if there is shear banding with one band weakly or not at all strained) a microscopic rearrangement at length scales of the cage (maximum cage deformation and/or restructuring) may results only to a small macroscopic strain (or deformation). For an amorphous solid under constant stress ($\sigma < \sigma_y$), the strain distribution may be heterogeneous in nature. Hence, there will be localized regions where cages are deformed stronger compared to others. This could lead to localized avalanches in colloidal glasses very similar to local fracture in metals. Such picture had been demonstrated by light scattering experiments for hard sphere glasses under stress.[33] Hence, such strain jumps maybe considered as the rheological fingerprints of the avalanches that are taking place in colloidal hard sphere glasses under constant stress. However, as mentioned, above such strain jumps are detected mainly in the younger glass indicative largely of a stochastic process that is more often found in a system with more shallow energy well landscape.[65]

Finally, we performed a very long-time (over 3 days) creep experiment. The rheometer was isolated by using a temperature isolation box around the rheometer oven, in order to investigate if external temperature fluctuations trigger such avalanches. Here, the temperature inside the isolation box as well as inside the oven (not shown here) are collected using a thermocouple as shown in Fig. 11. Despite the insulation we monitored some temperature fluctuations that are caused by fluctuation in the external environment. This is

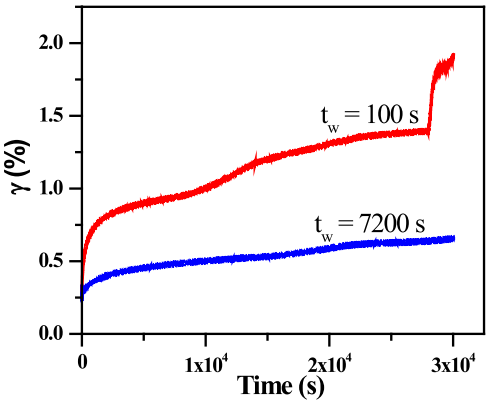

FIG. 10. Long-time creep experiments performed at two different waiting times after shear rejuvenation for $\sigma = 0.25$ Pa for a hard sphere colloidal glass with $\phi = 0.59$, $R = 106$ nm in squalene with yield stress, $\sigma_y = 2$ Pa.

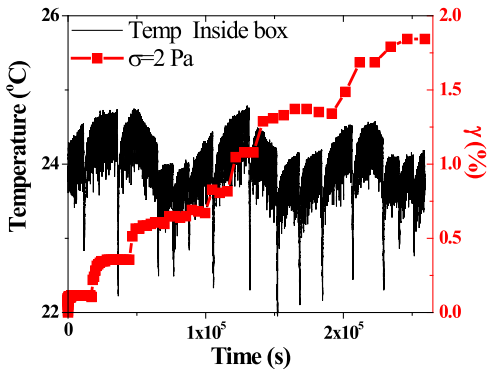

FIG. 11. Long-time creep experiments with $\sigma = 2$ Pa for a hard sphere colloidal glass with $\phi = 0.62$ and particle radius $R = 106$ nm in squalene performed on a DSR rheometer. The temperature fluctuations due to the surroundings are also noted.

reflected in a change in temperature of about 1.5 °C inside the box over time frame of the experiment. When $\sigma < \sigma_y$, we observe frequent strain jumps in the glass under constant stress. Although the strain jumps are not directly correlated with the fluctuations in temperature, the latter could be an external trigger for local avalanche type events that lead to macroscopic strain jumps during the creep test. This possibility needs to be thoroughly investigated by further experiments that are capable of providing detailed information on the microscopic structure, such as simultaneous rheometry and confocal experiments or by computer simulations.

IV. CONCLUSIONS

We have identified various rheological signatures of aging in the rheology of nearly hard sphere colloidal glasses. The effects of sample age on both linear and nonlinear viscoelastic properties of the glass were probed. The linear viscoelastic spectrum of the glass exhibits subtle changes during aging. At high Pe_ω, both elastic and viscous moduli do not change with sample age since short-time in-cage dynamics are age-independent. However, at intermediate/low Pe_ω, viscous modulus shows a slight decrease with sample age whereas the elastic modulus is not affected. Nonlinear rheological experiments such as start-up shear, creep and stress relaxation show discernible differences due to aging. The effect of aging in start-up shear flow experiments is manifested by an increase of stress overshoot peak. As the glass ages, it has an enhanced capability to retain larger stresses during stress relaxation experiments indicating a slowing-down of its intrinsic relaxation time. However, the effect of aging on stress relaxation is significantly reduced as the imposed strain overcomes the yield strain due to shear rejuvenation, which partially or fully erases aging effects. An aged glass creeps for a longer-period of time before steady state flow is reached due to slowing-down of relaxation time. We find that a shorter time with less work is required to induce yielding and flow during start-up shear rate experiments as compared to a switch-on stress (creep) experiment suggesting that faster particle dynamics take place during the transient period before reaching steady state in the former. Finally, abrupt strain jumps are detected during prolonged creep experiments for stresses below the yield stress and abrupt decay in stress during long time stress relaxation measurements. We associate such drastic changes of both strain and stress to plausible avalanche type phenomena during aging of a colloidal glass.

ACKNOWLEDGMENTS

The authors thank A. B. Schofield (University of Edinburgh) for providing the PMMA particles. This work was supported by Greek projects Thales Covisco, and Aristeia II MicroSoft, and EU project SmartPro.

REFERENCES

[1] R. Zargar, B. Nienhuis, P. Schall, and D. Bonn, "Direct measurement of the free energy of aging hard sphere colloidal glasses," Phys. Rev. Lett. **110**, 258301 (2013).
[2] Y. M. Joshi and G. Petekidis, "Yield stress fluids and ageing," Rheol. Acta **57**, 521–549 (2018).
[3] Y. M. Joshi, "Dynamics of colloidal glasses and gels," Annu. Rev. Chem. Biomol. Eng. **5**, 181–202 (2014).
[4] L. C. E. Struik, *Physical Aging in Amorphous Polymers and Other Materials* (Elsevier, 1978).
[5] G. B. McKenna, T. Narita, and F. Lequeux, "Soft colloidal matter: A phenomenological comparison of the aging and mechanical responses with those of molecular glasses," J. Rheol. **53**, 489–516 (2009).
[6] P. A. O'Connell and G. B. McKenna, "Large deformation response of polycarbonate: Time-temperature, time-aging time, and time-strain superposition," Polym. Eng. Sci. **37**, 1485–1495 (1997).
[7] C. A. Angell, K. L. Ngai, G. B. McKenna, P. F. McMillan, and S. W. Martin, "Relaxation in glass forming liquids and amorphous solids," J. Appl. Phys. **88**, 3113–3157 (2000).
[8] R. Angelini, E. Zaccarelli, F. De Melo Marques, M. Sztucki, A. Fluerasu, G. Ruocco, and B. Ruzicka, "Glass-glass transition during aging of a colloidal clay," Nat. Commun. **5**, 4049 (2014).
[9] N. Koumakis, A. B. Schofield, and G. Petekidis, "Effects of shear induced crystallization on the rheology and ageing of hard sphere glasses," Soft Matter **4**, 2008–2018 (2008).
[10] M. Bellour, A. Knaebel, J. L. Harden, F. Lequeux, and J.-P. Munch, "Aging processes and scale dependence in soft glassy colloidal suspensions," Phys. Rev. E **67**, 031405 (2003).
[11] M. Kaushal and Y. M. Joshi, "Linear viscoelasticity of soft glassy materials," Soft Matter **10**, 1891–1894 (2014).
[12] L. C. Johnson, E. Moghimi, G. Petekidis, and R. N. Zia, "Influence of structure on the linear response rheology of colloidal gels," J. Rheol. **63**, 583–608 (2019).
[13] N. Koumakis and G. Petekidis, "Two step yielding in attractive colloids: Transition from gels to attractive glasses," Soft Matter **7**, 2456–2470 (2011).
[14] A. Fluerasu, A. Moussaïd, A. Madsen, and A. Schofield, "Slow dynamics and aging in colloidal gels studied by x-ray photon correlation spectroscopy," Phys. Rev. E **76**, 010401 (2007).
[15] N. Koumakis, E. Moghimi, R. Besseling, W. C. K. Poon, J. F. Brady, and G. Petekidis, "Tuning colloidal gels by shear," Soft Matter **11**, 4640–4648 (2015).
[16] E. Moghimi, A. R. Jacob, N. Koumakis, and G. Petekidis, "Colloidal gels tuned by oscillatory shear," Soft Matter **13**, 2371–2383 (2017).
[17] W. van Megen, T. C. Mortensen, S. R. Williams, and J. Müller, "Measurement of the self-intermediate scattering function of suspensions of hard spherical particles near the glass transition," Phys. Rev. E **58**, 6073–6085 (1998).
[18] V. A. Martinez, G. Bryant, and W. van Megen, "Slow dynamics and aging of a colloidal hard sphere glass," Phys. Rev. Lett. **101**, 135702 (2008).
[19] V. A. Martinez, G. Bryant, and W. van Megen, "Aging dynamics of colloidal hard sphere glasses," J. Chem. Phys. **133**, 114906 (2010).
[20] G. Brambilla, D. El Masri, M. Pierno, L. Berthier, L. Cipelletti, G. Petekidis, and A. B. Schofield, "Probing the equilibrium dynamics of colloidal hard spheres above the mode-coupling glass transition," Phys. Rev. Lett. **102**, 085703 (2009).
[21] D. E. Masri, G. Brambilla, M. Pierno, G. Petekidis, A. B. Schofield, L. Berthier, and L. Cipelletti, "Dynamic light scattering measurements in the activated regime of dense colloidal hard spheres," J. Stat. Mech.: Theory Exp. **2009**, P07015.
[22] N. B. Simeonova and W. K. Kegel, "Gravity-induced aging in glasses of colloidal hard spheres," Phys. Rev. Lett. **93**, 035701 (2004).
[23] R. E. Courtland and E. R. Weeks, "Direct visualization of ageing in colloidal glasses," J. Phys.: Condens. Matter **15**, S359 (2003).
[24] S. Golde, T. Palberg, and H. J. Schöpe, "Correlation between dynamical and structural heterogeneities in colloidal hard-sphere suspensions," Nat. Phys. **12**, 712 (2016).
[25] W. Kob, F. Sciortino, and P. Tartaglia, "Aging as dynamics in configuration space," Europhys. Lett. **49**, 590 (2000).
[26] W. Kob, J. L. Barrat, F. Sciortino, and P. Tartaglia, "Aging in a simple glass former," J. Phys.: Condens. Matter **12**, 6385 (2000).
[27] M. Utz, P. G. Debenedetti, and F. H. Stillinger, "Atomistic simulation of aging and rejuvenation in glasses," Phys. Rev. Lett. **84**, 1471–1474 (2000).
[28] L. Ramos and L. Cipelletti, "Ultraslow dynamics and stress relaxation in the aging of a soft glassy system," Phys. Rev. Lett. **87**, 245503 (2001).
[29] L. Ramos and L. Cipelletti, "Intrinsic aging and effective viscosity in the slow dynamics of a soft glass with tunable elasticity," Phys. Rev. Lett. **94**, 158301 (2005).

[30]S. Mazoyer, L. Cipelletti, and L. Ramos, "Origin of the slow dynamics and the aging of a soft glass," Phys. Rev. Lett. **97**, 238301 (2006).
[31]O. Lieleg, J. Kayser, G. Brambilla, L. Cipelletti, and A. R. Bausch, "Slow dynamics and internal stress relaxation in bundled cytoskeletal networks," Nat. Mater. **10**, 236 (2011).
[32]N. Koumakis, M. Laurati, A. R. Jacob, K. J. Mutch, A. Abdellali, A. B. Schofield, S. U. Egelhaaf, J. F. Brady, and G. Petekidis, "Start-up shear of concentrated colloidal hard spheres: Stresses, dynamics, and structure," J. Rheol. **60**, 603–623 (2016).
[33]P. Ballesta and G. Petekidis, "Creep and aging of hard-sphere glasses under constant stress," Phys. Rev. E **93**, 042613 (2016).
[34]M. Siebenbürger, M. Ballauff, and T. Voigtmann, "Creep in colloidal glasses," Phys. Rev. Lett. **108**, 255701 (2012).
[35]Y. M. Joshi, "A model for aging under deformation field, residual stresses and strains in soft glassy materials," Soft Matter **11**, 3198–3214 (2015).
[36]A. R. Jacob, A. S. Poulos, S. Kim, J. Vermant, and G. Petekidis, "Convective cage release in model colloidal glasses," Phys. Rev. Lett. **115**, 218301 (2015).
[37]E. Moghimi, J. Vermant, and G. Petekidis, "Orthogonal superposition rheometry of model colloidal glasses with short-ranged attractions," J. Rheol. **63**, 533–546 (2019).
[38]N. Koumakis, J. F. Brady, and G. Petekidis, "Complex oscillatory yielding of model hard-sphere glasses," Phys. Rev. Lett. **110**, 178301 (2013).
[39]P. Ballesta, R. Besseling, L. Isa, G. Petekidis, and W. C. K. Poon, "Slip and flow of hard-sphere colloidal glasses," Phys. Rev. Lett. **101**, 258301 (2008).
[40]P. Ballesta, G. Petekidis, L. Isa, W. C. K. Poon, and R. Besseling, "Wall slip and flow of concentrated hard-sphere colloidal suspensions," J. Rheol. **56**, 1005–1037 (2012).
[41]P. Ballesta, N. Koumakis, R. Besseling, W. C. Poon, and G. Petekidis, "Slip of gels in colloid–polymer mixtures under shear," Soft Matter **9**, 3237–3245 (2013).
[42]R. Besseling, L. Isa, P. Ballesta, G. Petekidis, M. E. Cates, and W. C. K. Poon, "Shear banding and flow-concentration coupling in colloidal glasses," Phys. Rev. Lett. **105**, 268301 (2010).
[43]N. Koumakis, A. Pamvouxoglou, A. Poulos, and G. Petekidis, "Direct comparison of the rheology of model hard and soft particle glasses," Soft Matter **8**, 4271–4284 (2012).
[44]N. J. Wagner and J. F. Brady, "Shear thickening in colloidal dispersions," Phys. Today **62**(10), 27–32 (2009).
[45]J. Mewis and N. J. Wagner, *Colloidal Suspension Rheology* (Cambridge Series in Chemical Engineering, 2012).
[46]E. H. Purnomo, D. van den Ende, J. Mellema, and F. Mugele, "Rheological properties of aging thermosensitive suspensions," Phys. Rev. E **76**, 021404 (2007).
[47]N. Koumakis, M. Laurati, S. U. Egelhaaf, J. F. Brady, and G. Petekidis, "Yielding of hard-sphere glasses during start-up shear," Phys. Rev. Lett. **108**, 098303 (2012).
[48]G. Petekidis, A. Moussaid, and P. N. Pusey, "Rearrangements in hard-sphere glasses under oscillatory shear strain," Phys. Rev. E **66**, 051402 (2002).
[49]J. M. Brader, M. Siebenbürger, M. Ballauff, K. Reinheimer, M. Wilhelm, S. J. Frey, F. Weysser, and M. Fuchs, "Nonlinear response of dense colloidal suspensions under oscillatory shear: Mode-coupling theory and Fourier transform rheology experiments," Phys. Rev. E **82**, 061401 (2010).
[50]M. Ballauff, J. M. Brader, S. U. Egelhaaf, M. Fuchs, J. Horbach, N. Koumakis, M. Krüger, M. Laurati, K. J. Mutch, G. Petekidis, M. Siebenbürger, T. Voigtmann, and J. Zausch, "Residual stresses in glasses," Phys. Rev. Lett. **110**, 215701 (2013).
[51]E. Moghimi, A. R. Jacob, and G. Petekidis, "Residual stresses in colloidal gels," Soft Matter **13**, 7824–7833 (2017).
[52]T. Sentjabrskaja, P. Chaudhuri, M. Hermes, W. Poon, J. Horbach, S. Egelhaaf, and M. Laurati, "Creep and flow of glasses: Strain response linked to the spatial distribution of dynamical heterogeneities," Sci. Rep. **5**, 1884 (2015).
[53]C. Baravian, G. Benbelkacem, and F. Caton, "Unsteady rheometry: Can we characterize weak gels with a controlled stress rheometer?," Rheol. Acta **46**, 577–581 (2007).
[54]J. Sprakel, S. B. Lindström, T. E. Kodger, and D. A. Weitz, "Stress enhancement in the delayed yielding of colloidal gels," Phys. Rev. Lett. **106**, 248303 (2011).
[55]T. Sentjabrskaja, J. Hendricks, A. R. Jacob, G. Petekidis, S. U. Egelhaaf, and M. Laurati, "Binary colloidal glasses under transient stress-and strain-controlled shear," J. Rheol. **62**, 149–159 (2018).
[56]G. Petekidis, D. Vlassopoulos, and P. N. Pusey, "Yielding and flow of sheared colloidal glasses," J. Phys.: Condens. Matter **16**, S3955 (2004).
[57]K. N. Pham, G. Petekidis, D. Vlassopoulos, S. U. Egelhaaf, W. C. K. Poon, and P. N. Pusey, "Yielding behavior of repulsion- and attraction-dominated colloidal glasses," J. Rheol. **52**, 649–676 (2008).
[58]C. E. Maloney and A. Lemaître, "Amorphous systems in athermal, quasistatic shear," Phys. Rev. E **74**, 016118 (2006).
[59]N. P. Bailey, J. Schiøtz, A. Lemaître, and K. W. Jacobsen, "Avalanche size scaling in sheared three-dimensional amorphous solid," Phys. Rev. Lett. **98**, 095501 (2007).
[60]A. Lemaître and C. Caroli, "Rate-dependent avalanche size in athermally sheared amorphous solids," Phys. Rev. Lett. **103**, 065501 (2009).
[61]J. L. Barrat and A. Lemaître, "Heterogeneities in amorphous systems under shear," in *Dynamical Heterogeneities in Glasses, Colloids and Granular Media* (Oxford Science Publications, 2011).
[62]V. Chikkadi, "Spatial correlations and deformation modes in sheared colloidal glasses," Ph.D. thesis, Institute of Physics, University of Amsterdam, 2011.
[63]J. Weiss and D. Marsan, "Three-dimensional mapping of dislocation avalanches: Clustering and space/time coupling," Science **299**, 89–92 (2003).
[64]P. Coussot, Q. D. Nguyen, H. T. Huynh, and D. Bonn, "Avalanche behavior in yield stress fluids," Phys. Rev. Lett. **88**, 175501 (2002).
[65]E. Sanz, C. Valeriani, E. Zaccarelli, W. C. K. Poon, M. E. Cates, and P. N. Pusey, "Avalanches mediate crystallization in a hard-sphere glass," Proc. Natl. Acad. Sci. U. S. A. **111**, 75–80 (2014).